

NASA TECHNICAL NOTE



NASA TN D-4279

C. 1

NASA TN D-4279



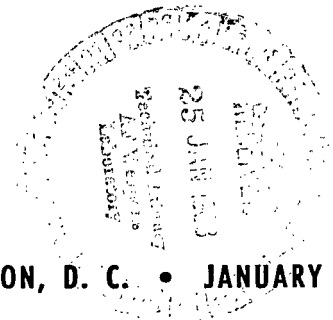
TECH LIBRARY KAFB, NM

LOAN COPY: RETU  
AFWL (WLIL-2  
KIRTLAND AFB, N

ESTABLISHING ALLOWABLE TEMPERATURE  
GRADIENTS FOR TUNGSTEN - URANIUM  
DIOXIDE FUEL ELEMENTS USING  
EXPERIMENTAL CYCLIC STRAIN DATA

*by Ivan B. Fiero*

*Lewis Research Center  
Cleveland, Ohio*



NATIONAL AERONAUTICS AND SPACE ADMINISTRATION • WASHINGTON, D. C. • JANUARY 1968



0130919

ESTABLISHING ALLOWABLE TEMPERATURE GRADIENTS FOR  
TUNGSTEN - URANIUM DIOXIDE FUEL ELEMENTS  
USING EXPERIMENTAL CYCLIC STRAIN DATA

By Ivan B. Fiero

Lewis Research Center  
Cleveland, Ohio

NATIONAL AERONAUTICS AND SPACE ADMINISTRATION

---

For sale by the Clearinghouse for Federal Scientific and Technical Information  
Springfield, Virginia 22151 - CFSTI price \$3.00

# ESTABLISHING ALLOWABLE TEMPERATURE GRADIENTS FOR TUNGSTEN - URANIUM DIOXIDE FUEL ELEMENTS USING EXPERIMENTAL CYCLIC STRAIN DATA

by Ivan B. Fiero  
Lewis Research Center

## SUMMARY

Fuel elements of nuclear reactors are inherently subjected to thermal gradients caused by surface cooling of a material with internal heat generation. These gradients may be cyclic in nature due to transient conditions imposed by changes in power demand or by multiple restarts of the reactor. Temperature distributions in the reactor fuel elements can vary from highly localized temperature perturbations to uniform variations in temperature over the entire structure. The highest thermal strain will result from the localized temperature perturbation and, consequently, a relatively small temperature difference can be tolerated. Higher temperature differences can be allowed if the temperature variations are less localized; that is, a thermal gradient which varies uniformly through a fuel element only produces one-half the thermal strain of a local temperature perturbation.

For a given temperature profile, the temperature difference necessary to produce a given strain is strongly dependent on variations with temperature of the coefficient of expansion of the material. The coefficient for tungsten - uranium dioxide cermets, for example, increases linearly with temperature. This behavior increases the thermal strain in the fuel material, and the calculated temperature difference required to produce a given strain is lower than if an average value for the coefficient of expansion were used.

To establish allowable limits for temperature differences in tungsten - uranium dioxide fuel elements, experimental thermal strain data were examined. The data were obtained by uniformly heating tungsten and tungsten - uranium dioxide composites for 50 thermal cycles. Since the materials were not cycled to failure, the allowable temperature differences established from the experimental data are not absolute maximum values, but represent design values with which fuel element configurations can be evaluated. These "allowable" temperature differences are those which would produce thermal strains equivalent to the experimental data. If the strains calculated for a given design are less than the experimental values, the fuel element should operate satisfactorily under the conditions considered.

## INTRODUCTION

Nuclear reactor fuel elements and core structural materials are subjected to many sources of stress. Inherent among these are thermal stresses, which can result, for example, from cooling the surface of a material in which heat is generated internally. These stresses and the corresponding thermal strains are frequently cyclic due to variations in the operating power level and multiple restarts of the reactor. High operating temperatures complicate the evaluation of such cyclic strains because of the detrimental effect of a lowered yield strength combined with the beneficial effect of an increased ductility.

In designing components for nuclear reactors, it is desirable to know the relation between the allowable thermal strain of a given material and the temperature difference which may be encountered during reactor operation. The purpose of this report is to establish such a relation for tungsten and tungsten - uranium dioxide materials based on the result of the experimental thermal strains reported in reference 1. Specimens used in these tests were not cycled to failure; hence, the data represent feasible rather than maximum strain limits. The "allowable" temperature difference established from these data can then be compared to the calculated temperature differences of various fuel element or structural geometries to determine if the thermal strains of a particular design are less than the values which have been experimentally proven to be feasible.

## CALCULATION OF THERMAL STRAIN

### Strains for Various Geometries

Thermal strains in reactor components result from a difference in temperature and/or differences in the coefficient of expansion. When the differences in the coefficient of expansion are neglected and no bending is assumed, the thermal strain is determined from

$$\epsilon = \alpha \Delta T \quad (1)$$

In a homogeneous material, a strain caused by a temperature gradient depends on the temperature difference through the material and on the shape of the temperature profile. Several specific types of temperature profiles are generally of interest for a nuclear reactor.

(1) Localized "hot spot" temperature perturbations may be caused by local deviations in fuel loading, fuel element thickness, etc. The resulting thermal strain (for a constant

coefficient of expansion) is essentially equal to the differential expansion between the local area and surrounding material, that is, equal to the maximum differential expansion

$$\epsilon = \alpha(T_{\text{avg}} - T_{\text{loc}}) \quad (2a)$$

or

$$\epsilon = \alpha \Delta T_{\text{max}} \quad (2b)$$

(2) Parabolic temperature profiles in flat plate and rod geometries result from internal heat generation with surface cooling. The thermal strain at any point in the material is proportional to the difference between the local expansion and the average expansion and must, therefore, be evaluated by integration of the temperature profile. For a constant coefficient of expansion, this difference can be expressed in terms of differences between local and average temperatures. For a flat plate with internal heat generation, for example, the maximum temperature difference between local and average temperature is equal to two-thirds of the maximum temperature difference existing in the material. Therefore, the maximum strain is

$$\epsilon = \frac{2}{3} \alpha \Delta T_{\text{max}} \quad (3)$$

Similarly, for a rod-shaped fuel element the maximum strain is proportional to one-half the maximum temperature difference in the material. The thermal strain is, therefore,

$$\epsilon = \frac{1}{2} \alpha \Delta T_{\text{max}} \quad (4)$$

(3) Linear or uniform temperature gradients would occur for heat conduction through a material with unequal surface temperatures. As in the previous cases, the maximum thermal strain can be related to the maximum temperature difference in the material. For a flat plate with a constant coefficient of expansion, maximum thermal strain is found to be

$$\epsilon = \frac{1}{2} \alpha \Delta T_{\text{max}} \quad (5)$$

When the thermal strains for flat plates for the three gradient conditions (eqs. (2b),

(3), and (5)) are compared, it is obvious that the first and third types of profiles produce the highest and lowest thermal strain. The thermal strain for the parabolic temperature distribution falls in between the other cases. In fact, all other possible temperature distributions would fall between the extremes of equations (2b) and (5). Therefore, only the temperature profiles that result in the highest and lowest strains need be considered since the limits established will bracket the entire range of interest.

## Effect of Variable Coefficient of Expansion

It was assumed in the previous discussion that the coefficient of expansion was constant. For a material with a coefficient of expansion that varies with temperature, the resulting strain relations are somewhat different than those defined by equations (2b), (3), (4), and (5). The relations are derived in appendix A for the case where the coefficient varies linearly with temperature; that is,

$$\alpha = K + K'T \quad (6)$$

The thermal strain for the localized temperature perturbation is given by

$$\epsilon = \Delta T_{\max} (K + 2K'\bar{T}) \quad (7)$$

where the mean temperature  $\bar{T}$  is

$$\bar{T} = \frac{T_1 + T_2}{2}$$

For the uniform temperature gradient, the relation for thermal strain in a flat plate is given by (appendix A)

$$\epsilon = \pm \frac{1}{2} \Delta T_{\max} (K + 2K'\bar{T}) - \frac{1}{6} K' \Delta T_{\max}^2 \quad (8a)$$

The plus and minus variation of the first term in this expression (eq. (8a)) indicates the maximum value of the tensile and compressive strains that occur at opposite surfaces of the flat plate. The expression also holds for a rod-shaped fuel element with a parabolic temperature profile where the plus and minus indicate the strain at the surface and center of the fuel element. Evaluation of equation (8a) shows that by neglecting the second-order term  $((1/6) K' \Delta T_{\max}^2)$  the error in determining the thermal strain is less than 3 percent

in range of  $\Delta T_{\max} = 550^{\circ} \text{C}$  and  $\bar{T} = 2200^{\circ} \text{C}$ . Neglecting this term yields the following approximate solution for a flat plate:

$$\epsilon = \frac{1}{2} \Delta T_{\max} (K + 2K'\bar{T}) \quad (8b)$$

Equations (7) and (8b) represent the highest and lowest strains for all possible temperature profiles within a flat plate.

Comparing equations (7) and (8b) indicates that the thermal strain for the localized temperature perturbation (eq. (7)) is twice that for the uniform gradient (eq. (8b)). This is the same factor which was previously determined for the constant coefficient of expansion (i. e., eqs. (2b) and (5)). However, for both the localized perturbation and uniform gradient, the strain for a given  $\Delta T_{\max}$  is greater than that which resulted for the constant coefficient. The effect of a thermal coefficient of expansion which is strongly increasing with temperature is, therefore, to decrease the temperature difference necessary to obtain a given strain. Of course, this conclusion can be reached qualitatively since the effect of a variable coefficient is to create an additional strain which must be superimposed on that resulting from a differential temperature.

## Cladding Considerations

The presence of a clad of another material on the surface of a fuel element would result in an additional strain in the clad due to the effect of dissimilar coefficients of expansion. If it was assumed that the clad was very thin compared to the fueled material, the strain would be

$$\epsilon_c = (\alpha_f - \alpha_c) T_c \quad (9)$$

where  $\alpha_f$  and  $\alpha_c$  are the coefficients of expansion of the fuel and clad material, and  $T_c$  is the temperature of the clad-fuel interface. The strain  $\epsilon_c$  must be added to the strain  $\epsilon$  calculated using equation (7) or (8b) to obtain the total strain in the clad.

## Thermal Strains in Tungsten and Tungsten - Uranium Dioxide Composites

When the previously discussed equations are used, the thermal strain in any material can be determined as a function of the temperature difference  $\Delta T_{\max}$  and mean temperature  $\bar{T}$  provided that the coefficient of expansion is known. Thermal expansion

coefficients of different compositions of fueled and unfueled tungsten as a function of temperature can be obtained from reference 1. The pertinent data are given in detail in appendix B. The compositions of the fueled materials involved are as follows:

Composite	Composition
I	90 vol. % W + 10 vol. % $\text{UO}_2$
II	80 vol. % W + 20 vol. % $\text{UO}_2$
III	70 vol. % W + 30 vol. % $\text{UO}_2$

It was found that the thermal expansion of composite I was virtually identical to unfueled tungsten. Thermal strain of all three composites were expressed as second-degree polynomials (ref. 1) for a temperature range of  $25^\circ \text{C} < T < 2500^\circ \text{C}$ :

Composite I:

$$\epsilon = 3.978 \times 10^{-5} + 3.591 \times 10^{-6} T + 9.870 \times 10^{-10} T^2 \quad (10)$$

Composite II:

$$\epsilon = -5.585 \times 10^{-5} + 4.319 \times 10^{-6} T + 1.027 \times 10^{-9} T^2 \quad (11)$$

Composite III:

$$\epsilon = -1.214 \times 10^{-4} + 3.457 \times 10^{-6} T + 1.610 \times 10^{-9} T^2 \quad (12)$$

The thermal coefficients of expansions may be obtained by taking the first derivative

$$\alpha = \frac{d\epsilon}{dT} \quad (13)$$

or, for composites I, II, and III, respectively,

$$\alpha = 3.591 \times 10^{-6} + 1.974 \times 10^{-9} T \quad (14)$$

$$\alpha = 4.319 \times 10^{-6} + 2.054 \times 10^{-9} T \quad (15)$$



$$\alpha = 3.457 \times 10^{-6} + 3.220 \times 10^{-9} T \quad (16)$$

where these coefficients of expansion are of the form  $\alpha = K + K'T$  as given in equation (6).

These coefficients of expansion may be utilized in the strain equations (7) and (8b). Calculated temperature differences  $\Delta T_{\max}$  for unfueled tungsten and fueled (80 vol. % W + 20 vol. %  $\text{UO}_2$ ) tungsten are shown in figures 1(a) and (b), respectively, as functions of the strain  $\epsilon$  for various mean temperatures  $\bar{T}$ . The coefficient of expansion for composite I was used for unfueled tungsten. Note that the calculated temperature difference  $\Delta T_{\max}$  is higher at low mean temperatures because the thermal coefficient of expansion is lower.

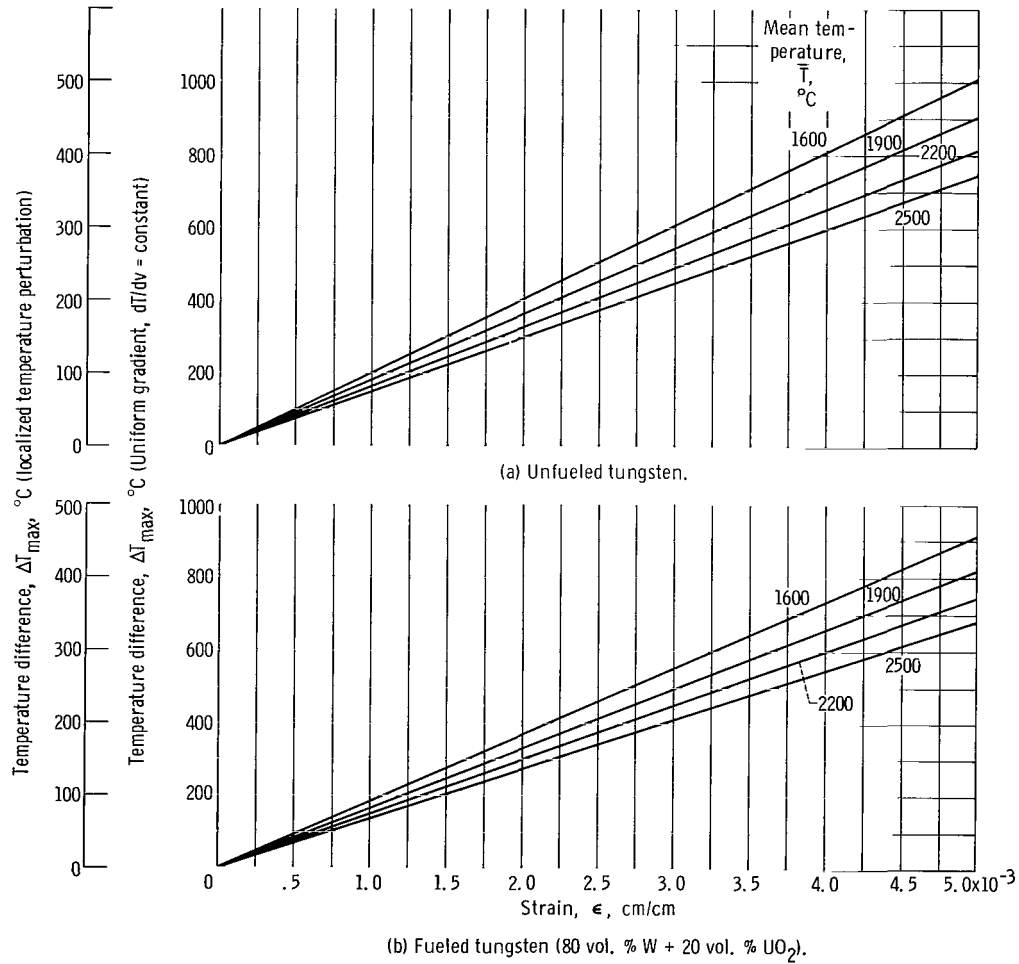


Figure 1. - Analytical temperature difference as function of strain for uniform gradient and a localized temperature at various mean temperatures.

## ALLOWABLE TEMPERATURE DIFFERENCES BASED ON EXPERIMENTAL STRAINS

Both unfueled tungsten and fueled tungsten composites were subjected to cyclic thermal strains as presented in reference 1. These strains were induced by elevating the temperature of two dissimilar bonded materials. One of the materials was of negligible cross-sectional area compared with the cross-sectional area of the second material. The strain is proportional to the difference in coefficient of expansion. These strains obtained without a temperature gradient can be interpreted as equivalent to strains that would result from a thermal gradient in a homogeneous material. The equivalent temperature difference for a particular gradient is that which will result in the same strain as the experimental strain.

### Experimental Strains

Strains were induced in two materials (ref. 1), (1) unfueled tungsten and (2) fueled (80 vol. % W + 20 vol. %  $\text{UO}_2$ ) tungsten. These two test materials were each bonded to fueled tungsten composites which had equal or higher coefficients of expansion. Composition and geometry of the test specimens are given in detail in appendix B. Figure 2 is a schematic of the geometry, and the following summarizes the combinations of materials used in the test specimens:

Specimens	Core material	Sleeve material
A	Composite I	Tungsten
B	Composite II	Tungsten
C	Composite III	Tungsten
D	Composite III	Composite II

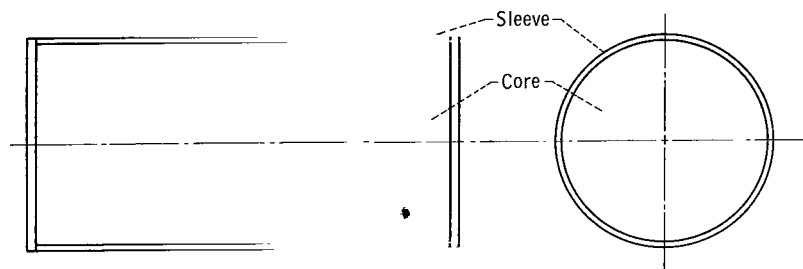


Figure 2. - Schematic of test specimens.

The sleeve is of negligible cross section as compared with the core. The core thereby serves as a means of cyclically straining the test materials (i. e. , the sleeve) a known amount. This amount depends on the difference in coefficient of expansion of each material and the temperature to which each test specimen was heated. Note that specimens A, B, and C will result in different strain levels on the same material, tungsten. The temperature was elevated from room temperature to 2500<sup>0</sup> C for a total of 50 cycles without cracking of any of the specimens. The strains, as calculated from the coefficient of expansion for a temperature increase to 2500<sup>0</sup> C, are listed in table I.

Four each of specimens A, B, and C and three of the D specimens were fabricated. Two each of specimens A, B, and C were held for 60 minutes at 2500<sup>0</sup> C; all the others were held for only 10 minutes.

Unfortunately, the actual strain in the specimens at 2500<sup>0</sup> C did not remain at the constant value listed in table I throughout the cyclic history of the specimen. The test specimens exhibited a variation in diametral and longitudinal dimensions as the cycling progressed. The room temperature diameter decreased and the length increased as discussed in appendix B. It is assumed that the fueled core alone caused the apparent dimension change and that the tungsten sleeve must strain to follow the core. Since the room temperature diameter after a number of cycles is less than the initial diameter, an increase in temperature to 2500<sup>0</sup> C must result in a smaller strain level than in the initial cycles. This lower strain would occur whether the strain is elastic, plastic, or a combination of both. Similarly, the longitudinal strain must increase. The change in room temperature dimensions as reported in reference 1 must be used to obtain a more accurate definition of the strain level actually experienced by the sleeve material. This

TABLE I. - STRESS PRODUCING STRAIN WITHIN THE SLEEVE AT  
2500<sup>0</sup> C CALCULATED FROM FREE THERMAL EXPANSION

(BASED ON THERMAL EXPANSION DATA)

Specimens	Composition		Free thermal expansion of core, $\epsilon_c$	Free thermal expansion of sleeve, $\epsilon_s$	Stress producing strain, $\epsilon$ , ( $\epsilon_c - \epsilon_s$ )
	Core	Sleeve			
A	I	Tungsten	$1.52 \times 10^{-2}$	$1.52 \times 10^{-2}$	$0.00 \times 10^{-2}$
B	II	Tungsten	1.72	1.52	.20
C	III	Tungsten	1.86	1.52	.34
D	III	<sup>a</sup> II	1.86	1.72	.14

<sup>a</sup>Coated with a thin layer of vapor deposited tungsten.

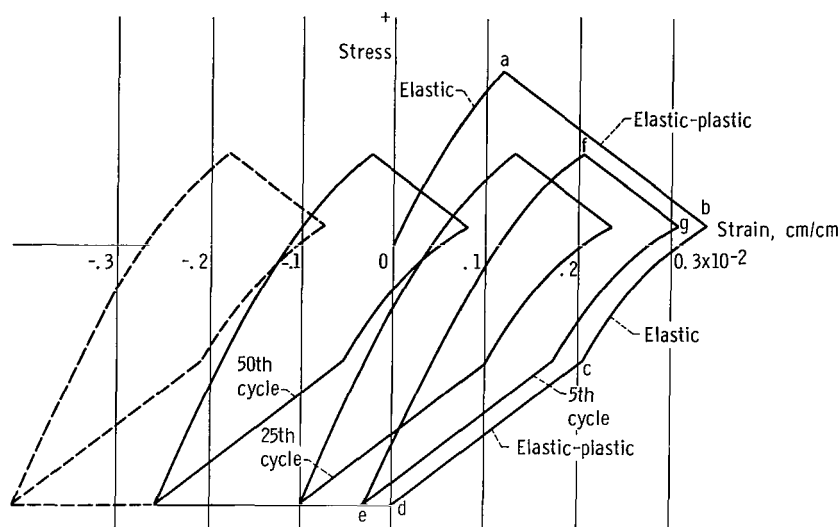


Figure 3. - Stress-strain diagram of sleeve for typical specimen. (Specimen C-8, tungsten sleeve, and 70 vol. % W + 30 vol. %  $UO_2$  core.)

can be accomplished by examining what happens to the stress-strain diagram as cycling progresses.

A typical example of the diametral decrease in sleeve strain is shown in figure 3. (The stress is somewhat uncertain due to unknowns such as yield strength and creep rates.) As the specimen begins its first thermal cycle, elastic strain in the sleeve increases until the yield stress is reached (point a). Further strain must be plastic. Since the yield stress also decreases as the temperature rises, the stress-strain path must slope downward to point b at  $2500^{\circ}\text{C}$  as shown in the figure. A considerable amount of plastic strain takes place and some of the elastic strain is relieved. The strain at point b corresponds to the calculated difference in free thermal expansion between the core and sleeve. These values were given in table I for all the combinations of materials.

As the temperature is decreased, the stress in the material must be relieved elastically until the compressive yield strength is reached at point c. The sleeve material continues to follow the thermally contracting core, yielding in compression at continually increasing stresses since the material yield strength increases as it cools. The residual core shrinkage is assumed to occur at the end of the cycle (after point d), whereas it probably is a gradual effect over the complete cycle. However, the final strain state for the assumed path corresponds to that of the actual path. At the end of the first cycle, the sleeve is in a state of compressive stress and strain due to inelastic strains at elevated temperature and core diametral shrinkage. For most of the specimens, the diameter continued to decrease as the number of cycles increased. After 5 cycles the diameter has decreased to point e as shown in figure 3.

As the temperature is again increased, the strain will be elastic until the yield stress is again reached. After the first cycle this strain occurs at a higher temperature and lower stress because the sleeve must first compensate for a negative residual stress. Consequently, the elastic portion continues to a point f in the positive stress-strain quadrant where yield begins. This point is displaced to the left from the line a-b an amount equal to the decrease in room temperature diameter. As the strain continues to increase, the stress must again follow an elastic-plastic strain path to point g. The stress-strain then follows a repetitive path with each succeeding cycle displaced an amount equal to the room temperature diameter decrease. The strain in the material on the 5th cycle, for example, goes from  $-0.03 \times 10^{-2}$  to  $0.31 \times 10^{-2}$  centimeter per centimeter and on the 50th cycle from  $-0.25 \times 10^{-2}$  to  $0.09 \times 10^{-2}$  centimeter per centimeter. Some of the specimens experienced a strain which decreased from a positive to a negative strain at high temperature as indicated by the dashed curve of figure 3. The diametral strain level at temperature can be found by simply subtracting the room temperature diameter shrinkage from the value listed in table I.

The adjusted strains, which take into account the room temperature dimensional changes, are given in table II for each specimen in the range of 25 and 50 thermal cycles. These tabulated values represent the minimum strain that occurred during the 25 or 50 cycles. For example, the minimum strain for a range of 50 cycles as shown in figure 3 is  $0.09 \times 10^{-2}$  centimeter per centimeter. The minimum strain will be conservatively low when applying it to thermal gradients for the same number of cycles. Twenty-five cycles was chosen as an intermediate value of probable interest to a designer. The 25 cycles may either represent the first or the final 25 cycles, depending on which 25 cycles experienced the highest strain level. For these calculations, it was assumed that the core shrinkage had no effect on its coefficient of expansion.

Similarly, the increase in longitudinal dimension accompanying cycling always tends to increase the longitudinal strain above that for the ideally stable core. Part of the increase in length, however, could be attributed to a swelling, or increase in thickness, of the specimen end cap. Estimates of end cap swelling and measured overall changes in the longitudinal dimensions of the specimens were used to estimate the actual longitudinal strains listed in table II. The end cap estimates were considered to be a maximum only, and consequently, only the growth of the specimen up to this maximum could be attributed to swelling.

The tungsten - uranium dioxide composite sleeve specimens did not have such end caps and any change in length must be the result of a core change. In addition, it may be possible that a composite sleeve would experience the same amount of additional sintering as the core; the diametral and longitudinal strains are then the theoretical strains based on the difference in coefficient of expansion listed in table I. This would only be characteristic of the D specimens and is included in table II.

TABLE II. - LONGITUDINAL AND DIAMETRAL STRAINS IN TUNGSTEN - URANIUM  
DIOXIDE CERMETS ADJUSTED FOR DIMENSIONAL INSTABILITY

Specimen	Hold time at temperature, min.	Number of cycles	Longitudinal and diametral strain from coefficient, $\alpha$	Adjusted strains		Biaxial strain ratio, $\epsilon_L/\epsilon_D$
				Diametral strain, $\epsilon_D$ , min.	Longitudinal strain, $\epsilon_L$ , min.	
A-7	10 ↓	25	$0.00 \times 10^{-2}$	$-0.19 \times 10^{-2}$	$-0.00 \times 10^{-2}$	0.00
A-15		25	.00	-.35	.16	-.46
B-10		25	.20	.10	.20	2.00
B-10		50	.20	.06	.20	3.34
B-12		25	.20	-.21	.20	-.95
C-7		25	.34	.34	.34	1.00
C-7		50	.34	.32	.34	1.06
C-8		25	.34	.24	.34	1.42
C-8		50	.34	.09	.34	3.78
A-8	60 ↓	25	$0.00 \times 10^{-2}$	$-0.49 \times 10^{-2}$	$0.59 \times 10^{-2}$	-1.20
A-10		↓	.00	-.29	.20	-.69
B-14		↓	.20	-.35	.20	-.57
B-19		↓	.20	-.19	.61	-3.22
C-9		↓	.34	-.04	.96	-24.00
C-10		↓	.34	-.16	.68	-4.25
$b_D$ -2	10 ↓	25	$0.14 \times 10^{-2}$	$0.11 \times 10^{-2}$	$0.14 \times 10^{-2}$	1.27
$b_D$ -2		50	↓	.04	.14	3.50
$b_D$ -3		25	↓	.29	5.24	.18
$b_D$ -3		50	↓	.10	.14	1.40
$b_D$ -4		25	↓	.42	.56	1.33
$b_D$ -4		50	↓	.14	.14	1.00
All type D <sup>c</sup>		50	↓	.14	.14	1.00

<sup>a</sup>With end cap correction.

<sup>b</sup>Assuming only core material changes dimension.

<sup>c</sup>Assuming both core and sleeve material change dimensions at the same rate.

Table II then summarizes the strains to which the unfueled tungsten (specimens A, B, and C) and W - 20 volume percent  $UO_2$  (D specimens) sleeve materials were subjected for 25 and 50 thermal cycles to  $2500^\circ C$  without failure. These values can be used as an indication of material capability either directly in terms of strains experienced or can be translated into equivalent temperature differences ( $\Delta T_{max}$ ) to determine allowable values for fuel element structures.

## Allowable Temperature Difference

Since, for reactor structures and fuel elements, the temperature profile is usually known from heat transfer analysis, the strains listed in table II are of more direct value if converted into allowable temperature differences. Note that since the test specimens were not cycled to failure, the allowable temperature differences established from the test do not represent absolute maximum values, but are more of a design value based on demonstrated feasibility. These temperature differences are the maximum allowable order to remain within the corresponding strain level for the number of cycles listed. The equations developed previously for a localized temperature deviation and for a uniform gradient may be used for this purpose. These temperature differences in both cases represent an allowable temperature difference for that particular temperature profile. Table III is a summary of the allowable temperature differences for a mean temperature level  $\bar{T}$  of  $2500^{\circ}\text{C}$ . In addition, the number of specimens that successfully resisted each succeeding lower strain level are indicated along with the range of strains that these specimens represent. For example, at least 3 specimens of tungsten cycled for 50 thermal cycles are known to withstand an equivalent uniform gradient  $\Delta T_{\text{max}}$  of  $89^{\circ}\text{C}$ , whereas one of these same 3 specimens withstood at least an equivalent  $476^{\circ}\text{C}$ .

The applicability of these equivalent thermal gradients based on diametral strains as demonstrable allowable cyclic temperature differences for the materials tested at  $2500^{\circ}\text{C}$  depends on several factors:

- (1) Temperature gradients in operating fuel elements result in situations in which material is in both tension and compression at low and high temperature. Although the test specimens were exposed to both compressive and tensile stresses at high temperature, they experienced only compressive stresses at room temperature.
- (2) The strains associated with one-dimensional thermal gradients are biaxial strains of equal magnitude. This would generally be the case for operating reactor fuel elements where the thermal gradients are essentially one dimensional. Although equal biaxial strain was the goal of the test program, this was rarely achieved due to dimensional changes in the core during cycling. An examination of table II indicates that ratios of longitudinal strain to diametral strain varied from 3.78 to -24.0 and included some cases in which the value is essentially zero.
- (3) The tests indicate how much cyclic strain can be safely imposed on tested materials when the peak temperature is  $2500^{\circ}\text{C}$ . It is not certain that the same amount of cyclic strain could be withstood at very much lower or higher temperatures.

In presenting these results it is assumed that the ability to resist cyclic strain does not depend on the direction of the strain; that is, the test results are generally applicable to cyclic thermal gradients whether tensile or compressive stresses exist at room tem-

TABLE III. - ALLOWABLE TEMPERATURE DIFFERENCE  $\Delta T_{\max}$  NECESSARY TO PRODUCE  
STRAIN EQUIVALENT TO ADJUSTED EXPERIMENTAL DIAMETRAL STRAIN

Number of cycles	Number of specimens	Range, $ \epsilon_D $	Minimum, $ \epsilon_D $	Range, $\epsilon_L/\epsilon_D$	Allowable temperature difference, $^{\circ}\text{C}$	
					Localized perturbation	Uniform gradient
Hold time, 10 min; tungsten material; mean temperature, $\bar{T}$ , 2500 $^{\circ}\text{C}$						
50	1	$0.32 \times 10^{-2}$	$0.32 \times 10^{-2}$	1.06	238	476
50	2	$0.09 \times 10^{-2}$ to $0.32 \times 10^{-2}$	.09	1.06 to 3.78	67	134
50	3	.06 to .32	.06	1.06 to 3.78	45	89
25	1	$0.35 \times 10^{-2}$	.35	-0.46	260	520
	2	$0.34 \times 10^{-2}$ to $0.35 \times 10^{-2}$	.34	-.46 to 1.00	253	506
	3	.24 to .35	.24	-.46 to 1.42	179	357
	4	.21 to .35	.21	-.95 to 1.42	156	312
	5	.19 to .35	.19	-.95 to 1.42	141	283
	6	.10 to .35	.10	-.95 to 2.00	74	149
Hold time, 60 min; tungsten material; mean temperature, $\bar{T}$ , 2500 $^{\circ}\text{C}$						
25	1	$0.49 \times 10^{-2}$	$0.49 \times 10^{-2}$	-1.20	364	729
	2	$0.35 \times 10^{-2}$ to $0.49 \times 10^{-2}$	.35	-1.20 to -0.57	260	520
	3	.29 to .49	.29	-1.20 to -.57	216	431
	4	.19 to .49	.19	-3.22 to -.57	141	283
	5	.16 to .49	.16	-4.25 to -.57	119	238
	6	.04 to .49	.04	-24.00 to -.57	30	60
Hold time, 10 min; fueled tungsten (W-UO <sub>2</sub> ); mean temperature, $\bar{T}$ , 2500 $^{\circ}\text{C}$						
25	1	$0.42 \times 10^{-2}$	$0.42 \times 10^{-2}$	1.33	288	576
25	2	$0.29 \times 10^{-2}$ to $0.42 \times 10^{-2}$	.29	0.18 to 1.33	199	398
25	3	.11 to .42	.11	.18 to 1.33	75	151
50	1	$0.14 \times 10^{-2}$	.14	1.00	96	192
50	2	$0.10 \times 10^{-2}$ to $0.14 \times 10^{-2}$	.10	1.00 to 1.40	69	137
50	3	.04 to .14	.04	1.00 to 3.50	27	55
<sup>a</sup> 50	6	$0.14 \times 10^{-2}$	.14	1.00	96	192

<sup>a</sup>Assuming equal additional sintering of core and sleeve.



perature or at high temperature. The range of biaxial strain ratios is also given in table III.

As discussed previously, the temperature differences obtained from the heat transfer of the reactor structure or fuel elements can be compared directly with table III to determine whether or not the design is acceptable. If the mean temperature  $\bar{T}$  is other than  $2500^{\circ}\text{C}$ , then the temperature difference  $\Delta T$  must be calculated from either the strains in table II and equations (7) and (8b) or determined from figures 1(a) and (b) in conjunction with the  $\Delta T$  of table III. However, it is more convenient to use figures 1(a) and (b). The  $\Delta T_{\text{max}}$  of table III (for  $2500^{\circ}\text{C}$   $\bar{T}$ ) is located on the  $2500^{\circ}\text{C}$   $\bar{T}$  line and the allowable  $\Delta T_{\text{max}}$  at any other desired  $\bar{T}$  found on a constant strain line. If it is necessary to take the presence of a clad into account, then the strain in the clad  $\epsilon_c$  must be subtracted from the total strain  $\epsilon$  to obtain the strain that is allowed for the gradient; that is, the strain is found from  $\Delta T_{\text{max}}$  and  $\bar{T}$  and  $\epsilon_c$  is subtracted along a constant  $\bar{T}$  line. The resulting  $\Delta T_{\text{max}}$  is the temperature difference then allowed across the gradient.

For example, table II indicates the strain for specimen C-7 to be at least  $0.32 \times 10^{-2}$  centimeter per centimeter for 50 cycles without failure and table III shows that an unfueled tungsten component (represented by C-7) should be able to withstand 50 operating cycles during which a uniform temperature gradient of  $476^{\circ}\text{C}$  or a very local deviation of  $238^{\circ}\text{C}$  is experienced at a mean temperature of  $2500^{\circ}\text{C}$ . If some other temperature level is of interest, for example, a mean temperature  $\bar{T}$  of  $1600^{\circ}\text{C}$ , the temperature difference allowable (fig. 1(a)) for a uniform gradient is  $646^{\circ}\text{C}$  and for a localized deviation is  $323^{\circ}\text{C}$ . If a clad strain  $\epsilon_c$  (from eq. (31)) of  $0.10 \times 10^{-2}$  centimeter per centimeter is present, then the allowable temperature difference at  $2500^{\circ}\text{C}$  is  $327^{\circ}\text{C}$  rather than  $476^{\circ}\text{C}$ .

## CONCLUDING REMARKS

Based on experimental thermal strain data obtained by cycling tungsten and tungsten - uranium dioxide composites, allowable temperature differences required to produce equivalent thermal strains were determined (table III) for a localized temperature perturbation and for a uniform temperature gradient. These two types of temperature profiles result in the maximum and minimum thermal strains for the conditions of interest in most nuclear reactors. The allowable temperature difference for a local temperature perturbation is only one-half that for the case where the temperature gradient is uniform. Conversely, for a given temperature difference the thermal strain is twice as great for the localized "hot spot."

The effect of a coefficient of expansion which increases with temperature is to increase the thermal strain for a given  $\Delta T$ . Allowable temperature differences for a material with a varying coefficient are, therefore, less than if the coefficient of expansion were simply evaluated at some mean temperature.

Although the experimental data reflected a dimensional instability with repeated thermal cycling (e. g. , a decrease in diameter), it was possible to conservatively define the strain level for repeated cycling as the minimum strain that occurred during the cycling.

Since the test specimens were not cycled to failure, the allowable temperature differences established from the data are design values rather than absolute maximum values which would cause failure. The calculated  $\Delta T_{\max}$  as a function of strain for various temperature levels is graphically presented in figures 1(a) and (b) for the gradient extremes. Comparison with these two extreme values should enable the designer to evaluate a given fuel element geometry to determine if the thermal strain conditions are within the values shown experimentally to be feasible.

Lewis Research Center,  
National Aeronautics and Space Administration,  
Cleveland, Ohio, August 8, 1967,  
122-28-02-04-22.

## APPENDIX A

### DERIVATION OF STRAIN EQUATIONS FOR A VARIABLE COEFFICIENT OF EXPANSION

Strain relations for materials which have an expansion coefficient that increases with temperature reflect a higher strain than that which results from constant coefficient for a given temperature difference. If the variable coefficient of expansion is taken into account, then the variables which effect the strain are the temperature level, the temperature difference, and the shape of the temperature profile.

Temperature gradients that appear in nuclear reactor components result from internal heat generation within cylindrical and flat geometries and heat transfer through unfueled material. For a given temperature difference in the material, the limiting cases of maximum strain are associated with two temperature profiles: (1) the temperature change or gradient may be uniform, or (2) the temperature change is a local perturbation. These limits dictate the highest and lowest possible strain for the given temperature difference and all other variations in the shape of the profile will give a maximum strain which will be bracketed by these extremes. The local perturbation may be, for example, a hot spot due to local deviation in fuel loading, thickness, etc. The uniform gradient will depend on geometry and is defined as a constant rate of temperature change per volume change in the direction of the gradient; that is,  $dT/dv = \text{constant}$ . An example of a local temperature perturbation and uniform gradient for a flat plate is shown in figure 4.

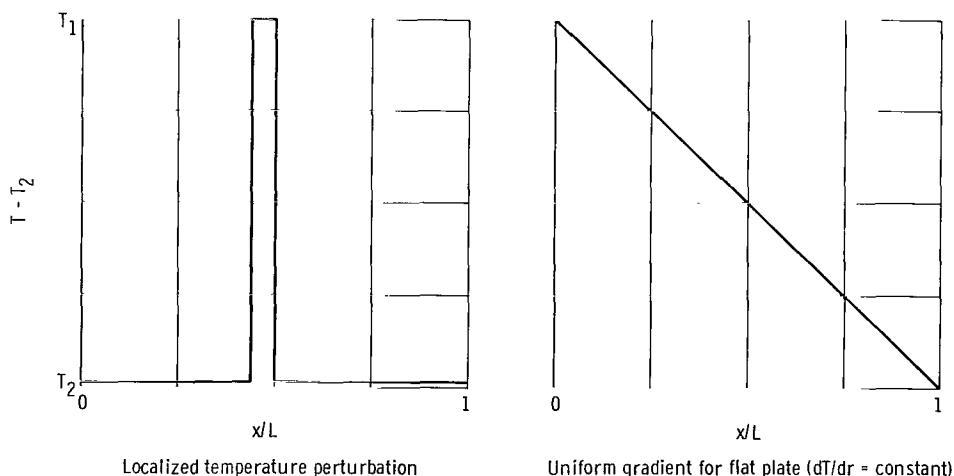


Figure 4. - Temperature gradients in nuclear reactor fuel elements for maximum and minimum thermal strains.

Thermal strain in the material is proportional to the difference between the local expansion and the average expansion. It is assumed that no bending of the fuel element takes place directly as a result of the gradient. Usually the inherent symmetry of the geometry prevents bending; if not, external restraints are provided to minimize bending.

### Localized Temperature Perturbation

In general, the strain is defined as

$$\epsilon = \alpha T \Big|_{\text{avg}} - \alpha T \quad (\text{A1})$$

if no bending of the geometry is allowed. For the case of a small localized temperature perturbation the average thermal expansion  $\alpha T \Big|_{\text{avg}}$  is

$$\alpha T \Big|_{\text{avg}} = \alpha_1 T_1$$

where essentially the bulk of the material is at temperature  $T_1$ . The maximum strain occurs within the point at temperature  $T_2$  and is

$$\epsilon = \alpha_1 T_1 - \alpha_2 T_2 \quad (\text{A2})$$

For a material which has a coefficient of expansion that is a linear function of temperature,

$$\alpha = K + K' T \quad (\text{A3})$$

The coefficient of expansion evaluated at  $T_1$  and  $T_2$  is

$$\alpha_1 = K + K' T_1 \quad (\text{A4})$$

and

$$\alpha_2 = K + K' T_2 \quad (\text{A5})$$

Substituting equations (A4) and (A5) into (A2) results in

$$\epsilon = (K + K' T_1) T_1 - (K + K' T_2) T_2 \quad (\text{A6})$$

or, rearrangement of the terms gives

$$\epsilon = K(T_1 - T_2) + K'(T_1 - T_2)(T_1 + T_2) \quad (\text{A7})$$

Define  $\Delta T$ , the temperature difference which can be applied to obtain the strain  $\epsilon$ , as

$$\Delta T \equiv T_1 - T_2 \quad (\text{A8})$$

and define the mean temperature as

$$\bar{T} \equiv \frac{T_1 + T_2}{2} \quad (\text{A9})$$

Substitution of  $\Delta T$  and  $\bar{T}$  into equation (A7) results in the strain

$$\epsilon = \Delta T(K + 2K'\bar{T}) \quad (\text{A10})$$

Equation (A10) can be used to evaluate the temperature difference  $\Delta T$  for the strain  $\epsilon$  at various mean temperature levels  $\bar{T}$ .

### Uniform Temperature Gradient

Similarly, for cases where the temperature variation is uniform, the strain can again be evaluated from

$$\epsilon = \alpha T \Big|_{\text{avg}} - \alpha T \quad (\text{A1})$$

where for a flat plate

$$\alpha T \Big|_{\text{avg}} \equiv \frac{\int_0^L \alpha T \, dx}{\int_0^L dx} = \frac{1}{L} \int_0^L \alpha T \, dx \quad (\text{A11})$$

Substituting  $(K + K'\bar{T})$  for the thermal expansion coefficient yields

$$\alpha T \Big|_{\text{avg}} = \frac{1}{L} \int_0^L (K + K' T) T \, dx \quad (\text{A12})$$

The temperature variation is defined as uniform and can be written

$$T = T_1 - \frac{x}{L} \Delta T \quad (\text{A13})$$

Substituting equation (A13) into (A12) and integrating result in

$$\alpha T \Big|_{\text{avg}} = K T_1 - K \frac{\Delta T}{2} + K' T_1^2 - K' \Delta T T_1 + K' \frac{\Delta T^2}{3} \quad (\text{A14})$$

From the definition of  $\Delta T$  and  $\bar{T}$ ,

$$T_1 = \bar{T} + \frac{1}{2} \Delta T \quad (\text{A15})$$

and

$$T_2 = \bar{T} - \frac{1}{2} \Delta T \quad (\text{A16})$$

Equation (A15) may be substituted into (A14) to obtain

$$\alpha T \Big|_{\text{avg}} = K \bar{T} + K' \bar{T}^2 + K' \frac{\Delta T^2}{12} \quad (\text{A17})$$

Evaluating  $\alpha T$  for the maximum tensile strain (at  $x/L = 1$ ) gives

$$\alpha_2 T_2 = (K + K' T_2) T_2 \quad (\text{A18})$$

or, substituting equation (A16) for  $T_2$  gives

$$\alpha_2 T_2 = K \bar{T} - \frac{1}{2} K \Delta T + K' \bar{T}^2 - K' \bar{T} \Delta T + \frac{K'}{4} \Delta T^2 \quad (\text{A19})$$

Finally, substituting (A17) and (A19) into (A1) gives

$$\epsilon_2 = \frac{1}{2} \Delta T(K + 2K'\bar{T}) - \frac{1}{6} K' \Delta T^2 \quad (A20)$$

Similarly, the maximum compressive strain (at  $x/L = 0$ ) can be solved for

$$\epsilon_1 = -\frac{1}{2} \Delta T(K + 2K'\bar{T}) - \frac{1}{6} K' \Delta T^2 \quad (A21)$$

An examination of equations (A20) and (A21) indicates an error, by neglecting the last term, of less than 3 percent in the range of  $\Delta T = 550^\circ \text{C}$  at  $\bar{T} = 2200^\circ \text{C}$ . Therefore, since the last term is small it may be neglected for these conditions, which gives the maximum tensile or compressive strain as

$$\epsilon = \frac{1}{2} \Delta T(K + 2K'\bar{T}) \quad (A22)$$

and the uniform thermal gradient results in one-half the strain resulting from that of a localized temperature perturbation.

Note that the resulting strain equations with a coefficient of expansion that increases with temperature produces a larger strain than that which would result from a constant coefficient of expansion. Evaluating the coefficient  $\alpha$  at a mean temperature  $\bar{T}$  would result in a considerable error, as can be seen from equations (A10) and (A22) where a factor of 2 is present in the temperature dependency term of the coefficient of expansion.

### Geometric Effect on Uniform Temperature Gradient

When the allowable temperature differences are applied in the analysis of fuel elements, fuel element geometry will affect the shape of the uniform temperature gradient. For example, a flat plate geometry would have a linear temperature profile. A cylindrical geometry, on the other hand, implies a parabolic profile because of the increase in volume per centimeter of radius ( $dT/dv = \text{constant}$ ).

From the definition  $dT/dv = \text{constant}$ , the temperature profile for a cylinder is found to be

$$T = T_1 - (T_1 - T_2) \frac{x^2}{L^2} \quad (A23)$$

where  $x$  is the variable distance from center and  $L$ , the length over which the gradient applies, is the radius of the cylinder.

The average thermal expansion will then be

$$\alpha T \Big|_{\text{avg}} \equiv \frac{\int_0^L \alpha T x \, dx}{\int_0^L x \, dx} = \frac{2}{L^2} \int_0^L \alpha T x \, dx \quad (\text{A24})$$

Evaluating the integral and finding the strain at  $T_1$  results in

$$\epsilon_1 = -\frac{1}{2} \Delta T (K + 2K' \bar{T}) - \frac{1}{6} K' \Delta T^2 \quad (\text{A25})$$

which is identical to equation (A21) for a flat plate.

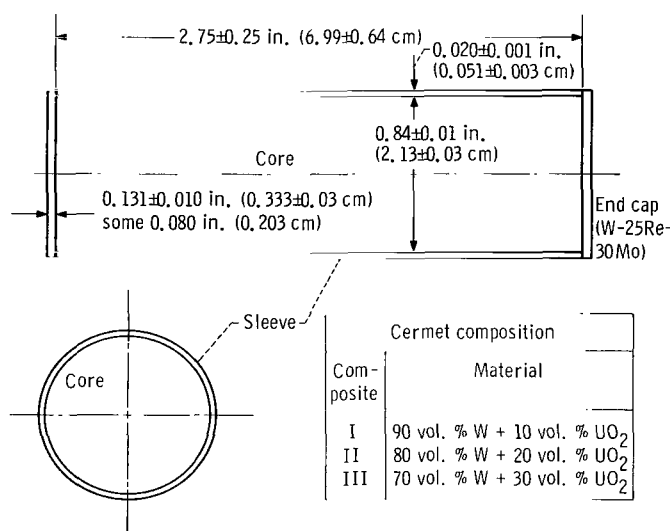
The appropriate temperature profile for other geometries may be found in a similar manner.



## APPENDIX B

### DESCRIPTION OF TUNGSTEN - URANIUM DIOXIDE COMPOSITES AND EXPERIMENTAL STRAIN DATA

Experimental data on cyclic thermal strains for tungsten - uranium dioxide composites were obtained from reference 1. The test specimens consisted of solid cylindrical cores with bonded sleeves and end caps. The cores were fabricated into a high density composite using agglomerated fuel particles blended with tungsten powder; the composite was cold-pressed and sintered. Cores were, on the average, 96 percent theoretical density. A sketch of the test specimens is given in figure 5. Three different compositions of the tungsten - uranium dioxide dispersions were used for the core. Composites were



Speci- mens	Specimen material				Sleeve material
	Diameter, in. (cm)	Length, in. (cm)	Sleeve thickness, in. (cm)	Core composite	
A	0.84 (2.13)	2.75 (6.99)	0.020 (0.051)	I	Tungsten
B	.84 (2.13)			II	Tungsten
C	.84 (2.13)			III	Tungsten
D <sup>a</sup>	.78 (1.98)			III	II <sup>b</sup>

<sup>a</sup>No end cap on D specimens.

<sup>b</sup>Fueled sleeve and end coated with 0.0015 ± 0.0005 in. (0.0038 cm) cladding of tungsten.

Figure 5. - Test specimen size and composition.

formed with 70, 80, and 90 percent tungsten and 30, 20, and 10 percent uranium dioxide, respectively. Detailed method of fabrication is given in reference 1. Thin sleeves were gas pressure bonded onto each of the three core types. Unfueled tungsten sleeves of vapor deposited tubes were cut to length and bonded onto the core. Other sleeves of fueled tungsten (80 vol. % W + 20 vol. %  $\text{UO}_2$ ) were machined from solid cylinders.

Four of each type of core composite were bonded with tungsten sleeves. Three specimens consisted of the fueled sleeve with a core composite of 70 volume percent W + 30 volume percent  $\text{UO}_2$ . The composite sleeves were coated with a very thin clad of fully dense unfueled tungsten to prevent fuel vaporization. End caps for all specimens except D specimens were made from W-25 atomic percent Re-30 atomic percent Mo alloy from a solid bar material. These end caps were gas pressure bonded into place at the same time that the sleeves were bonded to the core. Specimen D ends only had a thin coat of unfueled tungsten to prevent fuel vaporization.

Sintered specimens of each core composite were used for thermal expansion tests. Density of these expansion specimens and of the cyclic specimens is given in table IV.

TABLE IV. - CORE AND SLEEVE DENSITY OF  
TEST SPECIMENS

Specimen	Sintered density percent theoretical	
	Core	Sleeve <sup>a</sup>
A-7	96.6	100 ↓
B-12	96.0	
C-8	96.9	
A-15	96.8	
B-10	97.2	
C-7	96.9	
A-8	96.6	
B-14	95.8	
C-9	96.9	
A-10	96.5	
B-19	96.9	
C-10	96.7	
D-2	95.8	96.5
D-3	95.3	96.3
D-4	96.1	96.1
I-thermal expansion	96.5	(b)
II-thermal expansion	97.1	(b)
III-thermal expansion	95.5	(b)

<sup>a</sup>Sleeves of specimens A, B, and C are vapor deposited.

<sup>b</sup>Not applicable.

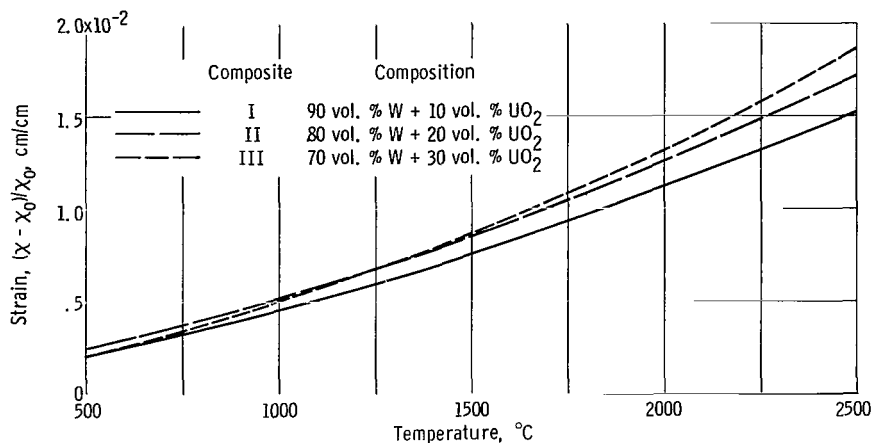


Figure 6. - Thermal expansion of tungsten - uranium dioxide composites.

A specimen of each type of core composite was run through several thermal cycles from room temperature to 2500° C to obtain data on the coefficient of linear thermal expansion (ref. 1). Measurements were made with an optical pyrometer and a micrometer microscope. The percent expansion as a function of temperature is presented in figure 6. Thermal expansion for unfueled tungsten was the same as for the 90 volume percent W + 10 volume percent UO<sub>2</sub> composite (ref. 1). All specimens were contained in a helium atmosphere.

A second-degree polynomial (ref. 1) was fit to the thermal expansion data yielding the following:

Type I:

$$\epsilon = 3.978 \times 10^{-5} + 3.591 \times 10^{-6}T + 9.870 \times 10^{-10}T^2$$

Type II:

$$\epsilon = -5.585 \times 10^{-5} + 4.319 \times 10^{-6}T + 1.027 \times 10^{-9}T^2$$

Type III:

$$\epsilon = -1.214 \times 10^{-4} + 3.457 \times 10^{-6}T + 1.610 \times 10^{-9}T^2$$

These equations are applicable for the temperature range of 25° to 2500° C.

Test cycling of the thermal specimens (ref. 1) consisted of a slow constant heating to 2500° C, a hold period, and a slow decrease to room temperature. Temperature was measured with an optical pyrometer at the higher temperatures. The time to tempera-

ture was 60 minutes and the time back to room temperature was approximately 200 minutes. All cycling was done in a helium atmosphere. Two hold periods were used. In one case, two each of specimens A, B, and C were cycled with a 10 minute hold; in the other case, two of each specimen type were cycled with a 60 minute hold. The specimens were checked every few cycles for possible cracking. A maximum of 50 cycles was imposed. Three D specimens were cycled with a 10 minute hold.

A change in room temperature dimensions of the specimens as a result of the thermal cycling was measured with a micrometer caliper during each inspection period. All of the specimens experienced a decrease in diameter and an increase in length (with an exception of the D specimens). The measured diametral and length changes are given in tables V to VII. It is believed that the decrease in diameter is, in part, due to additional sintering of the core material. For example, the measured core density of specimens B-12 and C-9 showed a definite increase from 96.0 and 96.9 to 97.6 and 99.4, respectively. An increase in porosity of the specimen end caps is responsible for some of the length growth. End cap material (W-25 at. % Re-30 at. % Mo) of thickness 0.080 and 0.131 inch (0.203 and 0.333 cm) were cycled for 50 cycles. Thickness increases in terms of the specimen length were 0.10 and 0.22 percent, respectively, both of which were less than the specimen longitudinal growth. A dissection of a cycled specimen showed an increase in the length of the fueled core itself. It is not known what caused this behavior. Consequently, it can reasonably be assumed that a biaxial strain condition exists in which the sleeve material strain is decreasing with cycling in the hoop direction and increasing with cycling in the longitudinal direction. Quantitatively, it would be conservative to neglect the increase in longitudinal strain. In any case, the minimum strain that the specimens were subjected to are the final diametrical strain (due to decreasing diameter) and initial longitudinal strain (due to increasing length).

TABLE V. - ROOM TEMPERATURE DIMENSION CHANGES

FOR UNFUELED SLEEVE WITH 10-MINUTE HOLD

Specimen	Number of cycles	Cumulative hours	Dimension change, cm/cm	
			Diametral	Longitudinal
A-7	5	22.5	$-0.08 \times 10^{-2}$	$0.00 \times 10^{-2}$
	10	45.0	-.14	-.02
	15	67.5	-----	-----
	20	90.0	-.17	.00
	25	112.5	-.19	↓
	27	121.5	-.21	
	29	130.5	-.21	
	32	144.0	-.23	
	34	153.0	-.24	
	36	162.0	-.23	.01
	38	171.0	-.24	.02
	40	180.0	-.25	.03
	45	202.5	-.26	.03
	50	225.0	-.26	.05
				.06
B-12	5	22.5	$-0.14 \times 10^{-2}$	$-0.04 \times 10^{-2}$
	10	45.0	-.23	-.04
	15	67.5	-----	-----
	20	90.0	-.35	.07
	25	112.5	-.41	.05
	27	121.5	-.43	.05
	29	130.5	-.46	.07
	32	144.0	-.47	.08
	34	153.0	-.47	.10
	36	162.0	-.50	.10
	38	171.0	-.51	.11
	40	180.0	-.52	.15
	45	202.5	-.54	.18
	50	225.0	-.56	.20
C-8	5	22.5	$-0.03 \times 10^{-2}$	$0.05 \times 10^{-2}$
	10	45.0	-.02	.14
	15	67.5	-----	-----
	20	90.0	-.14	.26
	25	112.5	-.10	.32
	27	121.5	-.17	-----
	29	130.5	-.19	.34
	32	144.0	-.19	.36
	34	153.0	-.21	.38
	36	162.0	-.21	.38
	38	171.0	-.22	.39
	40	180.0	-.23	.38
	45	202.5	-.26	.44
	50	225.0	-.25	.47

TABLE V. - Concluded. ROOM TEMPERATURE DIMENSION  
CHANGES FOR UNFUELED SLEEVE WITH  
10-MINUTE HOLD

Specimen	Number of cycles	Cumulative hours	Dimension change, cm/cm	
			Diametral	Longitudinal
A-15	5	22.5	$-0.13 \times 10^{-2}$	$0.10 \times 10^{-2}$
	10	45.0	-.21	.15
	15	67.5	-.27	.20
	20	90.0	-.32	.23
	25	112.5	-.35	.27
	30	135.0	-.37	.31
	35	157.5	-.39	.34
	40	180.0	-.42	.38
	45	202.5	-.43	.39
	50	225.0	-.45	.45
B-10	5	22.5	$0.02 \times 10^{-2}$	$0.04 \times 10^{-2}$
	10	45.0	.03	.09
	15	67.5	-.03	.13
	20	90.0	-.06	.17
	25	112.5	-.10	.19
	30	135.0	-.05	.28
	35	157.5	-.11	.38
	40	180.0	-.11	.33
	45	202.5	-.13	.36
	50	225.0	-.14	.40
C-7	5	22.5	$0.01 \times 10^{-2}$	$0.07 \times 10^{-2}$
	10	45.0	↓	.05
	15	67.5		.09
	20	90.0		.12
	25	112.5	.00	.12
	30	135.0	.00	.12
	35	157.5	.00	.14
	40	180.0	-.01	.15
	45	202.5	.00	.19
	50	225.0	-.02	.20

TABLE VI. - ROOM TEMPERATURE DIMENSIONAL  
CHANGES FOR UNFUELED SLEEVE WITH  
60-MINUTE HOLD

Specimen	Number of cycles	Cumulative hours	Dimension change, cm/cm	
			Diametral	Longitudinal
A-8	5	26.66	$-0.24 \times 10^{-2}$	$0.32 \times 10^{-2}$
	10	53.33	-.32	.43
	15	80.00	-.41	.51
	20	106.66	-.46	.56
	25	133.33	-.49	.64
	30	160.00	-.53	.65
	35	186.66	-.54	.78
	40	213.33	-.56	.75
	45	240.00	-.59	.84
	50	266.66	-.59	.83
B-14	5	26.66	$-0.28 \times 10^{-2}$	$-0.01 \times 10^{-2}$
	10	53.33	-.34	.00
	15	80.00	-.44	.00
	20	106.66	-.51	.02
	25	133.33	-.55	.05
	30	160.00	-.61	.06
	35	186.66	-.66	.10
	40	213.33	-.71	.12
	45	240.00	-.73	.15
	50	266.66	-.75	.19
C-9	5	25.66	$-0.14 \times 10^{-2}$	$0.42 \times 10^{-2}$
	10	53.33	-.28	.59
	15	80.00	-.31	.59
	20	106.66	-.36	.65
	25	133.33	-.38	.73
	30	160.00	-.42	.77
	35	186.66	-.44	.83
	40	213.33	-.47	.89
	45	240.00	-.48	.95
	50	266.66	-.50	1.00

TABLE VI. - Concluded. ROOM TEMPERATURE DIMEN-  
SIONAL CHANGES FOR UNFUELED SLEEVE  
WITH 60-MINUTE HOLD

Specimen	Number of cycles	Cumulative hours	Dimension change, cm/cm	
			Diametral	Longitudinal
A-10	5	26.66	$-0.13 \times 10^{-2}$	$0.04 \times 10^{-2}$
	10	53.33	-.19	.11
	15	80.00	-.21	.18
	20	106.66	-.29	.22
	25	133.33	-.29	.28
	30	160.00	-.32	.31
	35	186.66	-.33	.38
	40	213.33	-.35	.41
	45	240.00	-.35	.45
	50	266.66	-.35	.49
B-19	5	26.66	$-0.18 \times 10^{-2}$	$0.15 \times 10^{-2}$
	10	53.33	-.26	.23
	15	80.00	-.34	.30
	20	106.66	-.37	.41
	25	133.33	-.39	.49
	30	160.00	-.42	.54
	35	186.66	-.45	.59
	40	213.33	-.44	.66
	45	240.00	-.45	.76
	50	266.66	-.47	.81
C-10	5	26.66	$-0.18 \times 10^{-2}$	$0.22 \times 10^{-2}$
	10	53.33	-.29	.34
	15	80.00	-.35	.43
	20	106.66	-.48	.52
	25	133.33	-.50	.45
	30	160.00	-.56	.66
	35	186.66	-.61	.91
	40	213.33	-.65	.79
	45	240.00	-.67	.83
	50	266.66	-.71	.88



TABLE VII. - ROOM TEMPERATURE DIMENSIONAL CHANGES

FOR FUELED SLEEVE WITH 10-MINUTE HOLD

Specimen	Number of cycles	Cumulative hours	Dimension change, cm/cm	
			Diametral	Longitudinal
D-2	5	22.5	$-0.01 \times 10^{-2}$	$0.11 \times 10^{-2}$
	10	45.0	-.01	.11
	15	67.5	-.02	.07
	20	90.0	-.02	.08
	25	112.5	-.03	.09
	30	135.0	-.04	.10
	35	157.5	-.05	.10
	40	180.0	-.07	.11
	45	202.5	-.08	.13
	50	225.0	-.10	.16
<sup>a</sup> D-3	5	22.5	$-0.01 \times 10^{-2}$	$1.99 \times 10^{-2}$
	10	45.0	-.04	2.99
	15	67.5	.00	3.40
	20	90.0	.12	3.73
	25	112.5	.15	5.10
	30	135.0	.18	5.66
	35	157.5	.22	5.80
	40	180.0	.28	6.14
	45	202.5	.31	5.85
	50	225.0	.33	5.81
<sup>a</sup> D-4	5	22.5	$0.02 \times 10^{-2}$	$0.26 \times 10^{-2}$
	10	45.0	.13	.27
	15	67.5	.20	.33
	20	90.0	.24	.39
	25	112.5	.28	.42
	30	135.0	.33	.45
	35	157.5	.38	.47
	40	180.0	.43	.51
	45	202.5	.43	.54
	50	225.0	.46	.58

<sup>a</sup>Length strains for D specimens are unreliable because of blisters which formed for D-3 and D-4. D-2 is assumed reliable since no visible blisters formed.

## APPENDIX C

### SYMBOLS

K	coefficient of expansion at $T = 0^{\circ}\text{C}$ , $\text{cm}/(\text{cm})(^{\circ}\text{C})$	$\chi$	thermally expanded length of thermal expansion specimens
K'	slope of curve for coefficient of expansion, $[\text{cm}/(\text{cm})(^{\circ}\text{C})]/^{\circ}\text{C}$	$\chi_0$	initial reference length of thermal expansion specimens
L	dimension of material over which thermal gradient is applied	Subscripts:	
T	temperature, $^{\circ}\text{C}$	avg	average thermal expansion
$\bar{T}$	mean temperature, $^{\circ}\text{C}$	c	clad
$\Delta T$	temperature difference in thermal gradient, $^{\circ}\text{C}$	D	diametral
v	volume	f	fuel
x	coordinate for temperature profile	L	longitudinal
$\alpha$	linear coefficient of thermal ex- pansion, $\text{cm}/(\text{cm})(^{\circ}\text{C})$	loc	local
$\epsilon$	strain, $\text{cm}/\text{cm}$	1	values of parameters at location of maximum temperature
		2	values of parameters at location of minimum temperature

## REFERENCE

1. Conway, J. B.; and Collins, J. F.: Determination of the Resistance of Tungsten-UO<sub>2</sub> Composites to Cyclic Thermal Strains. General Electric Co. (NASA CR-72047), Aug. 30, 1966.

*"The aeronautical and space activities of the United States shall be conducted so as to contribute . . . to the expansion of human knowledge of phenomena in the atmosphere and space. The Administration shall provide for the widest practicable and appropriate dissemination of information concerning its activities and the results thereof."*

—NATIONAL AERONAUTICS AND SPACE ACT OF 1958

## NASA SCIENTIFIC AND TECHNICAL PUBLICATIONS

**TECHNICAL REPORTS:** Scientific and technical information considered important, complete, and a lasting contribution to existing knowledge.

**TECHNICAL NOTES:** Information less broad in scope but nevertheless of importance as a contribution to existing knowledge.

**TECHNICAL MEMORANDUMS:** Information receiving limited distribution because of preliminary data, security classification, or other reasons.

**CONTRACTOR REPORTS:** Scientific and technical information generated under a NASA contract or grant and considered an important contribution to existing knowledge.

**TECHNICAL TRANSLATIONS:** Information published in a foreign language considered to merit NASA distribution in English.

**SPECIAL PUBLICATIONS:** Information derived from or of value to NASA activities. Publications include conference proceedings, monographs, data compilations, handbooks, sourcebooks, and special bibliographies.

**TECHNOLOGY UTILIZATION PUBLICATIONS:** Information on technology used by NASA that may be of particular interest in commercial and other non-aerospace applications. Publications include Tech Briefs, Technology Utilization Reports and Notes, and Technology Surveys.

*Details on the availability of these publications may be obtained from:*

SCIENTIFIC AND TECHNICAL INFORMATION DIVISION  
NATIONAL AERONAUTICS AND SPACE ADMINISTRATION  
Washington, D.C. 20546